Author/s:
Feng, X;Zhang, P;Ng, K;Ajlouni, S;Liang, Z;Fang, Z

Title:
Peptidomics reveals enhanced bioactivities of hempseed cake induced by solid-state fermentation

Date:
2026-06-30

Citation:
Feng, X., Zhang, P., Ng, K., Ajlouni, S., Liang, Z. & Fang, Z. (2026). Peptidomics reveals enhanced bioactivities of hempseed cake induced by solid-state fermentation. Food Chemistry, 515, https://doi.org/10.1016/j.foodchem.2026.149243.

Persistent Link:
https://hdl.handle.net/11343/368687

Food Chemistry 515 (2026) 149243

Contents lists available at ScienceDirect

Food Chemistry

journal homepage: www.elsevier.com/locate/foodchem

Peptidomics reveals enhanced bioactivities of hempseed cake induced by solid-state fermentation

Xiaoyu Feng, Pangzhen Zhang, Ken Ng, Said Ajlouni, Zijian Liang, Zhongxiang Fang *

School of Agriculture, Food, and Ecosystem Sciences. Faculty of Science, The University of Melbourne, Parkville, Victoria 3010, Australia

ARTICLE INFO

Keywords:
Hempseed
Antioxidant
ACE inhibition
DPP-IV inhibition
Peptidomics
Molecular docking
Bioactive peptides

ABSTRACT

Novel peptides generated from solid-state fermented hempseed cake were characterized by peptidomics and validated for bioactivity. Fermentation with *Aspergillus niger*, *Bacillus subtilis*, and *Lactobacillus rhamnosus* markedly increased peptide numbers compared with the unfermented control and promoted the release of short peptides mainly from Cupin type-1 domain proteins, with leucine frequently occurring at cleavage termini. *In silico* prediction and molecular docking identified antioxidant, angiotensin-converting enzyme (ACE), and dipeptidyl peptidase-IV (DPP-IV) inhibitory candidates. Synthesized peptides confirmed that LDVSP and LVSPL showed potent ACE inhibition, with IC50 values of 107.47 ± 6.57 and 127.06 ± 12.11 μM, respectively, while LVSPL also inhibited DPP-IV (IC50 = 2.21 ± 0.04 mM). *B. subtilis* fermentation yielded the strongest antioxidant and ACE-inhibitory activities, whereas *A. niger* produced the highest DPP-IV inhibitory activity, highlighting fermented hempseed cake as a promising source of multifunctional bioactive peptides.

1. Introduction

Understanding and improving the nutritional quality of plant-based proteins has become increasingly important as global dietary patterns shift toward plant-based foods, driven by health, environmental, and ethical considerations (Wu et al., 2025). Among various sources, hempseed protein (*Cannabis sativa* L.) is recognized as a high-quality plant protein rich in essential amino acids and characterized by good digestibility (Leonard et al., 2021). Hempseed cake, a protein-rich by-product of oil extraction, remains relatively underexplored in terms of its nutritional and functional potential. Previous studies have demonstrated that hempseed protein hydrolysates possess diverse bioactivities, including antioxidant, angiotensin-converting enzyme (ACE) inhibitory properties, modulation of renal disease, reduction of hypercholesterolemia, inhibition of acetylcholinesterase, and regulation of glucose metabolism (Chen, Li, et al., 2023).

Traditional chemical and enzymatic hydrolysis methods can generate bioactive peptides but are often constrained by high costs, limited substrate specificity, and harsh processing conditions that may impair peptide functionality. In contrast, solid-state fermentation (SSF) is a well-established bioprocessing strategy widely used in food and biotechnology applications (Krishna, 2005; Pandey, 2003). Unlike single-enzyme hydrolysis, microorganisms in SSF secrete various extracellular proteases that act synergistically to hydrolyze complex plant matrices (Novelli et al., 2016). This process facilitates the release of low-molecular-weight peptides with potential bioactivity under mild and eco-efficient conditions (Feng et al., 2024; Wu et al., 2025).

Previous studies on hempseed proteins have primarily focused on protein extraction strategies and physicochemical characterization (Chen, Li, et al., 2023; Chen, Xu, et al., 2023). More recently, solid-state fermentation has been shown to enhance protein hydrolysis and bioactivity in hempseed cake (Feng et al., 2025). However, information on the peptide-level composition generated during fermentation and its relationship to observed bioactivities remains limited, and comprehensive peptidomic characterization of fermentation-derived peptides is still lacking.

This study utilizes high-resolution Orbitrap-based peptidomics and biochemical assays to determine if different microbial proteolytic systems generate distinct peptide profiles and bioactivity patterns from the same substrate. Hempseed cake was fermented using three microbial starters, *i.e.*, *Aspergillus niger* van Tieghem, *Bacillus subtilis* BSL1, and *Lactobacillus rhamnosus* GG, resulting in relatively low or high degrees of hydrolysis (DH) samples. While the enzymatic mechanisms were not directly investigated the enzyme mechanism, comparative peptidomic

* Corresponding author at: School of Agriculture, Food, and Ecosystem Sciences. Faculty of Science, The University of Melbourne, Parkville, Victoria 3010, Australia.
E-mail address: zhongxiang.fang@unimelb.edu.au (Z. Fang).

https://doi.org/10.1016/j.foodchem.2026.149243
Received 26 November 2025; Received in revised form 15 March 2026; Accepted 10 April 2026
Available online 13 April 2026

characteristics (peptide length, cleavage preference, and protein origin) are discussed as indirect indicators of microbial proteolytic behavior. Complementary biochemical assays for antioxidant, ACE, and human dipeptidyl peptidase-IV (DPP-IV) inhibitory activities were conducted to determine *in vitro* bioactivities, with lead peptide candidates further validated using chemically synthesized standards. Collectively, these findings provide insights into microbial fermentation strategies for enhancing the nutritional value of hempseed protein and highlight the importance of selecting appropriate starter cultures for the targeted production of bioactive peptides.

2. Materials and methods

2.1. Materials and reagents

Hempseed cake was supplied by Australian Primary Hemp (Geelong, VIC, Australia). *B. subtilis* BSL1 (ATCC 23857), *A. niger* van Tieghem (ATCC 16888) and L. *rhamnosus* GG (ATCC 53103) were procured from American Type Culture Collection (ATCC, Manassas, VA, USA). Synthesized peptides were purchased from Synpeptide Co., Ltd. (Shanghai, China). All remaining reagents, unless otherwise specified, were of analytical grade acquired from Sigma-Aldrich (Castle Hill, NSW, Australia).

2.2. Solid-state fermentation of hempseed cake

Hempseed cake was solid-state fermented with *A. niger*, *B. subtilis*, and L. *rhamnosus* as previously described (Feng et al., 2025). The DH was considered an outcome of fermentation rather than a controlled variable. For each microorganism, two representative fermentation conditions were selected and retrospectively classified as "L" (low DH) and "H" (high DH) based on their relative outcomes. These designations (ANL/ANH, BSL/BSH, and LRL/LRH) are intended for intra-microorganism comparisons only and do not indicate comparable absolute DH levels across different microbial species. The unfermented control (CON) consisted of autoclaved hempseed cake without inoculation. Detailed fermentation parameters and corresponding DH values are summarized in Table 1. The complete fermentation procedures were described previously (Feng et al., 2025).

2.3. Degree of hydrolysis

DH was determined using the 2,4,6-trinitrobenzene sulfonic acid (TNBS) assay, based on the method described by (Yu et al., 2023), with minor modifications. Fermented hempseed cake samples were mixed with 0.1 M PBS buffer (pH 7.4, 1:15 *w/v*), agitated at 140 rpm for 1 h, and centrifuged at 8000*g* for 10 min (Beckman Coulter Allegra V-15R, CA, USA) to collect the supernatant. For the assay, 25 μL of the supernatant was mixed with 200 μL pH 8.2 phosphate buffer and 200 μL 0.1% TNBS in capped tubes. The reaction mixture was incubated in a 50 °C water bath for 1 h. The reaction was terminated by adding 400 μL of 0.1 M HCl, and the absorbance was measured at 340 nm using a Thermo Scientific Varioskan LUX Multimode Microplate Reader (Thermo Fisher Scientific, Scoresby, VIC, Australia).

The total amino groups were determined using unfermented hempseed samples completely hydrolyzed with 6 M HCl at 120 °C for 24 h. The DH (%) was calculated using the equation:

$$DH(\%) = \frac{Asample - Ablank}{Atotal - Ablank} \times 100$$

where A_{Sample} represents the absorbance of the unfermented or fermented sample at 340 nm, A_{Blank} is the absorbance measured with deionized water in place of the sample, and A_{Total} is the absorbance of the completely hydrolysed sample.

Table 1
Fermentation conditions of hempseed cake.*

	Fermentation time (days)	Amount of added water (ml/g dw)	Inoculum size (spores/CFU /g dw)	Temperature (°C)	DH (%)
CON	–	–	–	–	2.75
ANL	5	1.2	1×10^6	26	15.67
ANH	7	0.8	1×10^7	26	33.61
BSL	7	1	1×10^7	26	35.80
BSH	9	0.8	1×10^7	26	48.72
LRL	5	1	1×10^8	37	33.28
LRH	9	1	1×10^6	37	45.63

* CON, unfermented hempseed cake; ANL/ANH, BSL/BSH, and LRL/LRH: hempseed cake fermented with *A. niger*, *B. subtilis*, and *L. rhamnosus* yielding relatively low (L) and high (H) degrees of hydrolysis, respectively. DH: degree of protein hydrolysis. L and H classifications represent relative outcomes within each specific microorganism and do not indicate comparable absolute DH values across different starter cultures. DH was determined using the TNBS method described in Section 2.3.

2.4. Fermented hempseed cake soluble protein extraction and ultrafiltration fractionation

Unfermented and fermented hempseed cakes were washed three times with methanol to remove phenolic compounds and residual oil. For each wash, the samples were mixed with methanol at a 1:20 (*w/v*) ratio, shaken for 1 h, and centrifuged to remove the supernatant. After the third wash, the residue was dried under a fume hood and extracted with Milli-Q water at a 1:20 (w/v) ratio, shaking at 140 rpm for 2 h on a platform shaker. The mixture was then centrifuged at 4000 ×*g* for 30 min at 4 °C.

The resulting supernatant was subjected to fractionation by ultrafiltration using a 3 kDa molecular weight cut-off (MWCO) membranes (Vivaspin® 20 centrifugal concentrator, Sartorius, Göttingen, Germany), to obtain the <3 kDa peptide fraction. Both the total soluble protein and the <3 kDa peptide fraction were lyophilized and stored at −20 °C for subsequent bioactivity assays.

2.5. Determination of protein content

Protein concentrations of the soluble extracts and their <3 kDa fractions were determined using the Pierce BCA Protein Assay Kit (23,225, Pierce™ BCA Protein Assay Kit, Thermofisher Scientific, San Jose, CA, USA) following the manufacturer's protocol, with bovine serum albumin (BSA) serving as the protein standard. For the <3 kDa fractions, the measured values are reported as BCA-equivalent concentrations and were used for comparative purposes among samples rather than as absolute peptide quantification.

2.6. Scanning electron microscopy

Dried hempseed powder samples were mounted on glass slides using double-sided adhesive carbon tape. The samples were coated with gold using a sputter coater (Emitech K550X, Quorum Technologies, Lewes, UK) prior to imaging. Micrographs were acquired with an electron probe microanalyser (JXA-8530F, JEOL, Tokyo, Japan) operated at an accelerating voltage of 15 kV. Representative images were obtained at magnifications of 250× and 5000×

2.7. LC-MS/MS acquisition for peptidomics

2.7.1. Sample preparation for peptidomics

The hempseed water extract (1:20, *w*/w) was filtered through a 3 kDa molecular weight cut-off centrifugal filter unit (Vivaspin® 500, Sartorius, Göttingen, Germany). The filtrate was freeze-dried, reconstituted in 1 mL of 0.1% (*v*/v) formic acid, and purified *via* solid-phase

extraction (SPE) using Oasis HLB cartridges (Waters Corporation, Milford, MA, USA). Briefly, the cartridges were conditioned with 1 mL of HPLC-grade acetonitrile (ACN), loaded with 1 mL of sample in 0.1% formic acid (FA), washed twice with 1 mL of 0.1% (v/v) trifluoroacetic acid (TFA), and eluted with 2 mL of 80% (v/v) ACN containing 0.1% (v/v) TFA. The eluted fraction was freeze-dried again and reconstituted in 2% acetonitrile with 0.05% TFA. To avoid ion suppression during electrospray ionization (ESI), LC–MS/MS analysis was performed using FA-based mobile phases, ensuring that residual TFA was effectively removed during the initial trap column loading phase. Prior to LC-MS/MS analysis, the solution was centrifuged at 13,000 rpm for 10 min.

2.7.2. LC-MS/MS analysis

Liquid chromatography was performed using label-free quantification (LFQ) on an Ultimate 3000 RSLCnano system (Thermo Fisher Scientific, Bremen, Germany) equipped with an Acclaim PepMap RSLC nano-trap column (75 μm × 2 cm, Thermo Fisher) and an analytical column (75 μm × 50 cm, Thermo Fisher), maintained at 50 °C. The mobile phases consisted of solvent A (water containing 5% *v*/v DMSO and 0.1% v/v formic acid) and solvent B (acetonitrile containing 5% v/v DMSO and 0.1% v/v formic acid). Peptides were separated at a flow rate of 300 nL/min using the following gradient: 3% B for 6 min, increased linearly to 23% B over 59 min, further to 40% B over 10 min, then to 80% B within 5 min, maintained at 80% B for 5 min, and finally returned to 3% B within 0.1 min followed by equilibration for 9.9 min.

Mass spectrometry was performed on an Orbitrap Eclipse Tribrid mass spectrometer (Thermo Fisher Scientific) operated in positive ion mode. Full MS scans (*m/z* 375–1500) were acquired at 120,000 resolution with an AGC target of 400,000. The most intense precursors (charge +2 to +7, intensity >50,000) were selected for HCD fragmentation (30% collision energy) with a 1.6 m/z isolation window, and MS/MS spectra were recorded at 15,000 resolution (AGC target 50,000). Data-dependent acquisition was applied with a 3 s cycle time and 30 s dynamic exclusion.

2.7.3. Peptide sequencing and screening

Peptides were identified using PEAKS Studio (version 11, Bioinformatics Solutions Inc., Waterloo, Canada) (Zhang et al., 2012). Raw files first underwent *de novo* peptide sequencing to generate candidate sequences directly from the MS/MS spectra. These sequences were subsequently used to assist database searching against integrated UniProt protein databases to ensure accurate identification. The control group (CON) was searched against the *Cannabis sativa* database (UP000583929, 30,192 entries). For fermented groups, combined databases were used: hemp plus *A. niger* (UP000253845), *B. subtilis* (UP000001570), or L. *rhamnosus* (UP000307517) (all accessed 30 July 2025).

Database searches were conducted without enzyme specificity to account for non-specific proteolysis during solid-state fermentation. Oxidation (M) and carboxymethylation (C) were included as variable post-translational modifications. Precursor and fragment mass tolerances were set to 10 ppm and 0.02 Da, respectively. Peptide–spectrum matches (PSMs) were filtered at a false discovery rate (FDR) of 1.0%. Proteins were accepted at $-10\,\mathrm{lgP} \geq 20$, and peptides were accepted at $-10\,\mathrm{lgP} \geq 15$. To ensure identification confidence, only peptides with an Average Local Confidence (ALC) greater than 90% were retained. Each sample was analyzed in triplicate, and only peptides detected in at least two replicates were included in the final dataset.

PeptideRanker (http://distilldeep.ucd.ie/PeptideRanker/) score peptides for potential bioactivity, with scores >0.5 considered indicative of potential biological relevance (Mooney et al., 2012). In addition, peptide sequences were compared against the BIOPEP-UWM database (https://biochemia.uwm.edu.pl/biopep-uwm/) to annotate potential biological activities, such as antioxidant, ACE-inhibitory, and DPP-IV inhibitory motifs (Minkiewicz et al., 2019).

2.8. Molecular docking of representative peptide on the ACE and DPP-IV binding sites

The top five most abundant peptides from each fermented sample were further analyzed through molecular docking to provide structural insights into peptide–enzyme interactions. Three-dimensional structures of the peptides were constructed using ChemDraw v20.0 and energy minimized. The crystal structures of the human ACE complexed with lisinopril (PDB ID: 1O8A) and human DPP-IV complexed with a selective inhibitor (PDB ID: 4A5S) were obtained from the RCSB Protein Data Bank (http://www.rcsb.org) (Burley et al., 2019). Protein preparation was performed using the Schrödinger Suite (version 2024-2, Schrödinger, LLC, New York, NY, USA), involving hydrogen bond refinement, addition of missing atoms, and removal of water molecules and atomic conflicts. The structures were optimized using the OPLS4 force field. Peptides were prepared *via* LigPrep/Epik (pH 7.0 ± 2.0), followed by OPLS4 minimization. Molecular docking was conducted using GLIDE module in extra precision (XP) mode. For ACE, the grid box was centred at x = 40.79, y = 33.61, and z = 43.38, covering the active site region that binds lisinopril (Wang et al., 2017). For DPP-IV, the grid box was defined around the catalytic binding sites (Glu205, Glu206, Tyr662, Tyr666, Tyr547, Trp629, Tyr631, Trp659, Ser630, Asp708, His740) with coordinates x = 18.82, y = 37.65, and z = 55.27 (Sutton et al., 2012). These coordinates represent the geometric center of the active sites as determined by the position of the native ligands or catalytic residues. Top poses were ranked by docking score (kcal/mol) and visualized in Maestro.

2.9. Peptide synthesis

Based on the molecular docking results, eight representative peptides (LFNP, LDVSP, LVSPL, FHLA, GNLF, DDRNSLLR, AFGALS, FDERLR) with high predicted binding affinity toward ACE or DPP-IV were selected for chemical synthesis and *in vitro* chemical validation. Peptides were synthesized by Synpeptide Co., Ltd. (Shanghai, China) using standard solid-phase peptide synthesis. Peptide purity (>98%) was confirmed by high-performance liquid chromatography (HPLC) as provided by the manufacturer. Lyophilized peptides were stored at −20 °C until further use and freshly dissolved in 50 mM pH 7.8 Tris-HCl buffer prior to bioactivity assays.

2.10. Antioxidant activity assays (ABTS and FRAP)

For bioactivity assays, peptide extracts were adjusted to an apparent concentration of 1 mg/mL based on BCA assay measurements. The antioxidant activity of the hempseed cake peptide extracts was evaluated using the 2,2′-azinobis-(3-ethylbenzothiazoline-6-sulfonate) (ABTS) radical scavenging and the ferric reducing antioxidant power (FRAP) assays.

The ABTS assay was conducted according to the method described by Cano et al. (1998) and subsequently modified by Leonard et al. (2021). A stock solution was prepared by mixing 7.4 mM ABTS with 2.6 mM potassium persulfate (1:1, *v*/v), which was kept in the dark for 12 h. The solution was then diluted with methanol to obtain a working solution with an absorbance of 1.1 ± 0.02 at 734 nm. An aliquot of 30 μL of peptide extract was added to 270 μL of ABTS working solution, vortexed for 30 s, and incubated for 15 min in the dark at room temperature. The absorbance was measured at 734 nm using a Thermo Scientific Varioskan LUX Multimode Microplate Reader. Trolox (6-hydroxy-2,5,7,8-tetramethylchroman-2-carboxylic acid) was used for the standard curve (0–0.1 mg) establishment. Results were expressed as milligrams of Trolox equivalents (TE) per milligram of protein or per gram of sample.

The FRAP assay was based on the method described by Griffin and Bhagooli (2004) and subsequently modified by Liang et al. (2024). FRAP reagent was freshly prepared by mixing acetate buffer (300 mM, pH 3.6), 20 mM $FeCl_3{\cdot}6H_2O$, and 10 mM TPTZ solution (in 40 mM HCl) at a

ratio of 10:1:1 (*v*/v/v). A 50 μL sample aliquot was mixed with 1 mL FRAP reagent and 0.45 mL Milli-Q water, incubated at 37 °C for 5 min in the dark, and then measured at 593 nm. Iron (II) sulfate heptahydrate (0–50 μM) was used to generate standard curve. Results were expressed as millimoles of Fe^{2+} equivalents per milligram of protein or per gram of sample.

2.11. ACE inhibition assay

ACE inhibitory activity was assessed following the method of Sonklin et al. (2020), with minor modifications. Briefly, ACE was extracted by suspending 0.1 g of rabbit lung acetone powder (Sigma-Aldrich, L0756) in 10 mL of 100 mM sodium borate buffer (pH 8.3) containing 5% (*v*/v) glycerol. The mixture was agitated at 140 rpm for 2 h and incubated overnight at 4 °C to obtain the enzyme extract. For the assay, 150 μL of 0.5 mM N-[3-(2-furyl)acryloyl]-*L*-phenylalanylglycine (FAPGG; Sigma-Aldrich, F5137) in 50 mM Tris-HCl buffer (pH 8.2) containing 0.3 M NaCl was mixed with 25 μL of ACE solution and 25 μL of the 1 mg/mL peptide extract (or various concentration of synthesized peptides). Purified ACE (Sigma, A6778, 50 mU/mL) was used for the validation of synthesized peptides to ensure high precision. The decrease in absorbance at 340 nm was recorded at 0 and 30 min at 37 °C using a Thermo Scientific Varioskan LUX Multimode Microplate Reader. Captopril (C4042, Sigma-Aldrich) was used as a reference inhibitor to validate the ACE inhibition assay. 50 mM pH 7.8 Tris-HCl buffer was used as a blank. The ACE inhibitory activity was calculated as follows:

$$ACE\ inhibition\ (\%) = \left(1 - \frac{slope\ of\ the\ sample\ curve}{slope\ of\ the\ blank\ curve}\right) \times 100$$

2.12. DPP-IV inhibition assay

DPP-IV inhibitory activity was determined based on the method described by Xie et al. (2024). 100 μL Tris-HCl buffer (50 mM pH 7.8), 25 μL of 1 mg/mL peptide extract (or various concentrations of synthesized peptide) and 50 μL of 50 mU/mL human DPP-IV (Sigma-Aldrich, D4943) were mixed and pre-incubated at 37 °C for 30 min. The reaction was initiated by adding 25 μL of substrate Gly-Pro-p-nitroanilide (1.6 mM) and incubated at 37 °C for 30 min. Both substrate and enzyme were prepared in 50 mM Tris-HCl buffer (pH 7.8). The absorbance was monitored at 405 nm using a Thermo Scientific Varioskan LUX Multimode Microplate Reader. Tris-HCl buffer (50 mM, pH 7.8) was used as a blank.

The DPP-IV inhibitory activity was calculated as:

$$DPPIV\ inhibition\ (\%) = \left(1 - \frac{slope\ of\ the\ sample\ curve}{slope\ of\ the\ blank\ curve}\right) \times 100$$

2.13. Data analysis

Except otherwise stated, each experiment was conducted in triplicates, and results are reported as the means ± standard deviations. Significant differences among sample means were determined *via* one-way ANOVA with Fisher grouping at a 95% confidence level ($p < 0.05$) using Minitab (Minitab 21.1.0, Sydney, Australia). Data visualization and curve fitting were performed using Origin 2024b (OriginLab Corporation, Northampton, MA, USA).

3. Results and discussion

3.1. Physicochemical characteristics of fermented hempseed cake

The soluble protein content of the fermented hempseed cake and the <3 kDa fraction are summarized in Table 2. Similar to previously reported (Feng et al., 2025), the soluble protein content increased significantly after fermentation, which can be attributed to the proteolytic activity of microbial enzymes converting insoluble proteins into soluble forms. A similar pattern was observed in the <3 kDa peptide-enriched fraction, with fermentation significantly increasing ($p < 0.05$) the content of low-molecular-weight peptides from 2.11 mg/g in the control (CON) to a maximum of 47.21 mg/g in the BSH. Correspondingly, the proportion of the <3 kDa peptide fraction relative to the total protein extract rose from 7.5% to 25.9%. These findings align with the expected role of fermentation in degrading high-molecular-weight proteins into smaller peptides. The notably higher production of low-molecular-weight peptides in the BSH group may be attributed to the efficient proteolytic system of *Bacillus subtilis* or its superior adaptation to the hempseed substrate (Oyeleke et al., 2011), compared with other two tested microorganism strains of *A. niger* and L. *rhamnosus*.

Table 2
Soluble protein content of fermented hempseed cake and peptide-enriched content of the <3 kDa fraction.*

Sample	Soluble protein (mg/g)	<3 kDa peptide fraction (mg/g, BCA-equivalent)	<3 kDa fraction/ Soluble protein Ratio (%)
CON	28.12 ± 0.7^{d}	2.11 ± 0.2^{e}	7.5
ANL	77.54 ± 9.3^{c}	13.56 ± 0.9^{d}	17.5
ANH	92.1 ± 6.3^{c}	20.28 ± 1.2^{c}	22.0
BSL	192.04 ± 9.9^{ab}	25.49 ± 1.3^{c}	13.3
BSH	182.41 ± 4.8^{b}	47.21 ± 3.8^{a}	25.9
LRL	199.38 ± 13.1^{ab}	36.93 ± 1.7^{b}	18.5
LRH	206.64 ± 9.9^{a}	36.25 ± 2.4^{b}	17.5

* Abbreviations (CON, ANL, ANH, BSL, BSH, LRL, LRH) are defined in Table 1. Values with different superscript letters within a column are significantly different ($p < 0.05$). Values for the <3 kDa fraction represent BCA-equivalent content of peptide-enriched fractions and are intended for comparative purposes.

The relationship between the DH and the production of <3 kDa peptides varied depending on the starter culture. In *A. niger* and *B. subtilis* fermentations, the high-DH groups (ANH and BSH) produced significantly higher amounts of <3 kDa peptides than their low-DH counterparts. This aligns with the general expectation that higher DH values correspond to more extensive protein degradation and increased peptide release. Similar results were reported in soybean curd fermented by *Mucor racemosus* MD-102 and *Lactobacillus plantarum* Lb-p1 (Wei et al., 2021). However, an opposite effect was observed for L. *rhamnosus*, where the high-DH group (LRH) yielded fewer <3 kDa peptides than the low-DH group (LRL). This finding suggests that, in L. *rhamnosus* fermentation, extended incubation (9 days in LRH *vs.* 5 days in LRL; Table 1) may have led to further hydrolysis of released peptides into free amino acids (FAAs). During prolonged fermentation, FAAs can be actively consumed by L. *rhamnosus* for growth and metabolism. Consistent with this dynamic process, our previous study using the same fermentation system reported lower residual FAA content in LRH than in LRL (Feng et al., 2025). Therefore, the reduced <3 kDa fraction content observed in LRH likely reflects the combined effects of peptide hydrolysis, microbial utilization, and intracellular metabolism rather than a single mechanism. A comparable trend was noted by *P.* wang and Ma (2024), who observed that peptide content in solid-state fermented buckwheat peaked at 48 h of fermentation with *Lactiplantibacillus plantarum* and subsequently declined with prolonged fermentation.

Scanning electron microscopy (SEM) was employed to observe microstructural changes in the hempseed cake following fermentation (Fig. 1). At magnification of 250× (Fig. 1a), fermented samples (ANH, BSH, LRH) appeared more dispersed compared to the unfermented sample (CON), with reduced particle size after fermentation. Similar observations have been reported for fermented soybean protein meal treated with *Lactobacillus plantarum* Lp6 (Amadou et al., 2010). The effects of fermentation were more pronounced at 5000× (Fig. 1b), where smaller particle sizes were evident, suggesting enhanced protein

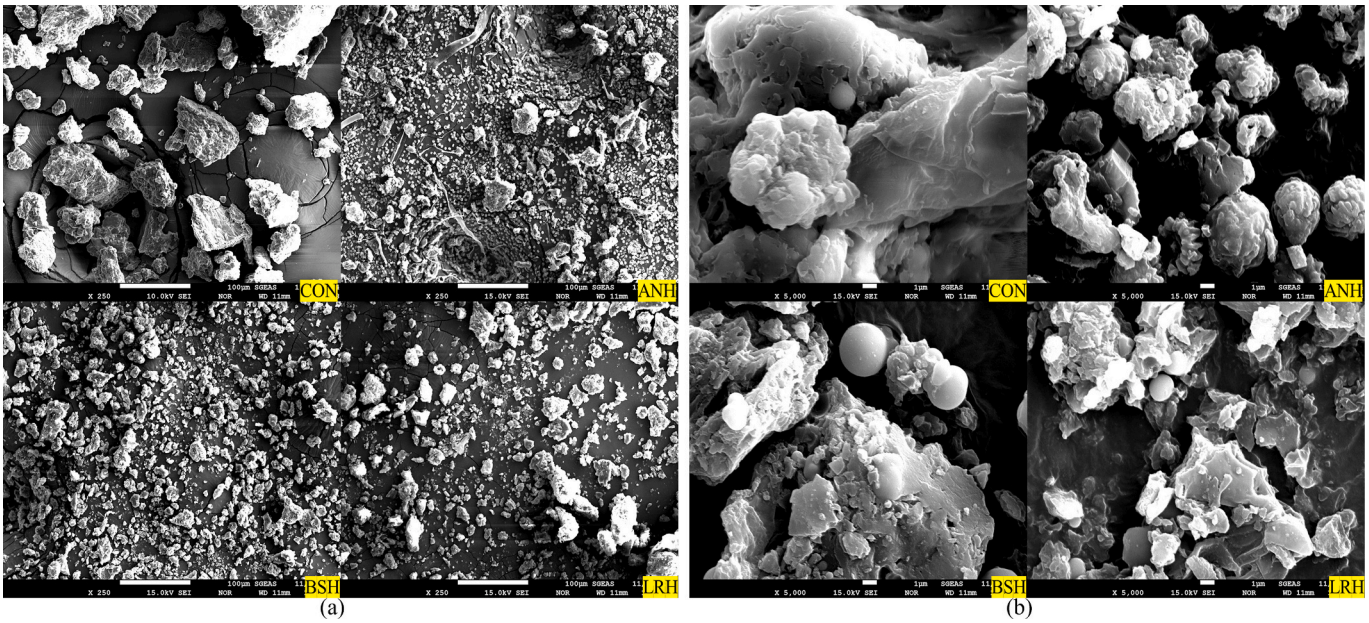

Fig. 1. Scanning electron micrographs of unfermented (CON) and fermented hemp seed cakes (ANH, BSH, and LRH refer to Table 1) in (a) 250× and (b) 5000× magnification. Small spherical structures indicated by the orange arrows were suggested as oil droplets.

exposure and extractability. Interestingly, small spherical structures indicative of oil droplets were observed. These droplets disappeared after *A. niger* fermentation but remained visible in *B. subtilis* and L. *rhamnosus* fermented samples. This aligns with previous findings that *A. niger* can hydrolyze lipids through the secretion of lipase enzymes (Alabdalall et al., 2021; Garcia et al., 2021).

3.2. Peptidomics of unfermented and fermented hempseed cake

3.2.1. Overall peptide profile and diversity

A peptidomics approach based on data-dependent acquisition (DDA), combined with a non-specific enzyme search against integrated proteome databases of hempseed (*Cannabis sativa*) and the corresponding microorganisms, enabled a comprehensive analysis of generated peptides.

All fermented groups exhibited markedly higher peptide counts and total peak area compared with the unfermented control (Table 3). Only 40 peptides were detected in the unfermented hempseed (CON), indicating limited endogenous proteolysis in the raw material. In contrast, the total number of identified peptides in fermented groups ranged from 696 in LRH to 1195 in BSH, with total peak area increasing by nearly two orders of magnitude compared with the CON. Among these, the *B. subtilis* (BS) group produced the most peptide diversity and abundance, with BSH showing the highest peptide count (1195) and peak area in the MS chromatography.

Across all fermented samples, peptides were predominantly short, with over 80% of sequences containing 4–9 amino acid residues (Table 3). The *B. subtilis*–fermented samples (BSL and BSH) exhibited the highest proportion of short peptides (4–6 residues), consistent with the strong proteolytic capacity of *Bacillus*-derived enzymes such as subtilisin and neutral protease (Contesini et al., 2018). Peptides comprising 2–9 amino acids are generally considered to possess enhanced bioavailability and with multifunctional bioactivities (Mooney et al., 2012).

Venn diagrams (Fig. 2a) indicated that, within the same starter culture, different DH (*i.e.*, fermentation conditions) resulted in distinct peptide profiles, with less than 50% overlap observed in the *A. niger* and *B. subtilis* groups. This indicates that the extent of proteolysis significantly influences the diversity of peptides generated. Such variations in peptide profiles under different fermentation conditions have also been reported in milk fermented by *Streptococcus thermophilus* and

Table 3
Number of certain length peptide and summed peak area of unfermented and fermented hempseed cake.*

Peptide length	CON	ANL	ANH	BSL	BSH	LRL	LRH
4	3	273	356	541	582	341	260
5		199	318	209	244	153	153
6	3	56	90	86	128	102	92
7	5	60	81	90	101	96	82
8	5	42	39	54	67	58	45
9	2	32	33	37	37	34	30
10	4	29	29	18	15	19	19
11	5	21	16	11	11	10	12
12	8	9	5	5	7	5	3
13		7	10		2	1	
14	2	2	4		1		
15	1	3	1				
16	1		1				
19	1						
Total number	40	733	983	1051	1195	819	696
Sumed peak area	3.17E+08	2.23E+10	3.99E+10	2.1E+10	5.47E+10	3.7E+10	1.82E+10

* Abbreviations (CON, ANL, ANH, BSL, BSH, LRL, LRH) are defined in Table 1.

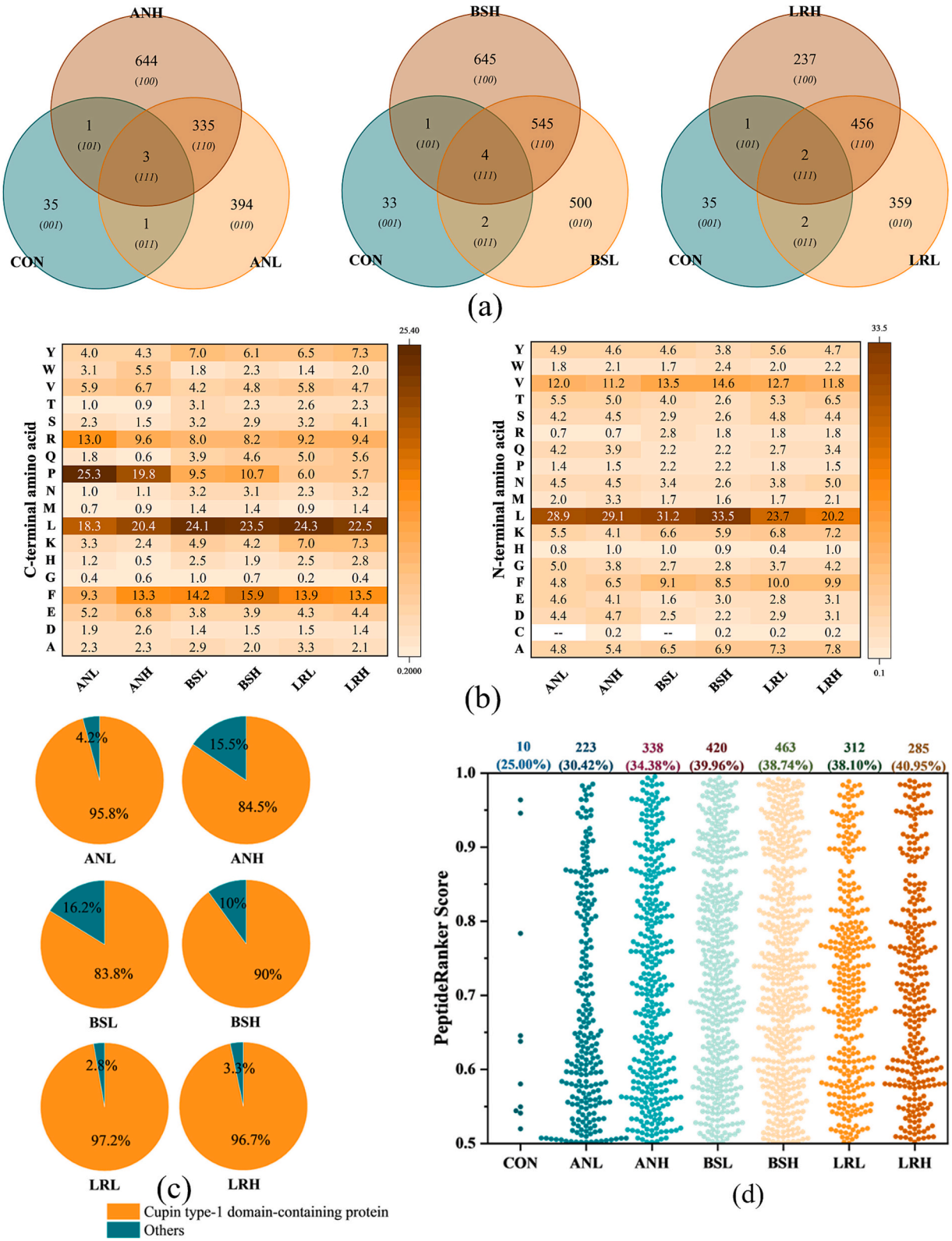

Fig. 2. Peptidomic analysis of unfermented (CON) and fermented hempseed cake samples (ANL/H, BSL/H, and LRL/H refer to Table 1). (a) Venn diagram showing the distribution of peptides identified in CON and fermented samples; (b) frequency of peptide cleavage sites at the C-terminal and N-terminal positions (A = alanine, C = cysteine, D = aspartic acid, E = glutamic acid, F = phenylalanine, G = glycine, H = histidine, K = lysine, L = leucine, M = methionine, N = asparagine, P = proline, Q = glutamine, R = arginine, S = serine, T = threonine, V = valine, W = tryptophan, Y = tyrosine); (c) precursor proteins of the identified peptides; and (d) PeptideRanker score distribution of predicted bioactive peptides. The numbers in the top X axis indicate the counts of predicted bioactive peptides, while the values in the parentheses represent the ratio of the bioactive peptides to the total detected peptides.

Lactobacillus bulgaricus (Yu et al., 2021).

3.2.2. Terminal amino acid frequencies

Terminal amino acid frequencies demonstrated distinct and microorganism-dependent cleavage preferences. Although glutamate is the most abundant amino acid in hempseed proteins, cleavage-site analysis showed that this background composition did not dominate the generated peptide (House et al., 2010; Wang et al., 2008). Instead, at the C-terminus, *A. niger* preferentially cleaved at proline (P) and leucine (L), whereas *B. subtilis* and L. *rhamnosus* predominantly generated peptides terminating in leucine (L) and phenylalanine (F) (Fig. 2b). At the N-terminus, all three microorganisms showed enrichment of leucine (L) and valine (V).

The preference for cleavage at these hydrophobic residues is likely associated with the distinct proteolytic systems secreted by each microorganism during fermentation. For example, *A. niger* produces prolyl endoproteinase, *B. subtilis* secretes subtilisin and carboxypeptidases, and *L. rhamnosus* expresses cell-envelope proteinases, all of which tend to cleave peptide bonds adjacent to hydrophobic amino acids (David Troncoso et al., 2022; Norris et al., 2014) (Solieri et al., 2018).

However, cleavage patterns are also substrate-dependent. For instance, *B. subtilis* fermentation of soybean meal typically results in C-terminal cleavage at leucine (L) and glutamic acid (E) (Kumari et al., 2023), whereas L. *rhamnosus* fermentation of soybean has been reported to favor arginine (R) at the C-terminus (Zhang et al., 2023). These differences suggest that protease specificity is influenced by both the microorganism and the protein substrate, highlighting the limited understanding of microbial cleavage behavior within the hemp protein matrix. The identity of terminal amino acids is a key determinant of peptide stability and biological activity. In particular, peptides containing proline (P), leucine (L), or valine (V) at the N- or C-terminus are frequently associated with strong ACE- and DPP-IV inhibitory activities, which may contribute to the bioactivities observed in the following sections (Ding et al., 2023; Mu et al., 2024).

3.2.3. Precursor protein origins

Fig. 2c shows the precursor proteins of the detected peptides. In all fermented samples, most peptides originated from cupin type-1 domain–containing proteins (83.8–97.2%). The predominance of Cupin-derived peptides likely reflects both the high abundance of these storage proteins in hempseed and their susceptibility to microbial proteolysis during fermentation (Gao et al., 2021). Phylogenetically, these proteins represent canonical members of the Cupin superfamily, which is characterized by a conserved β-barrel structural motif and is functionally associated with plant seed storage and secondary metabolism (Dunwell et al., 2000). Within this superfamily, the Edestin family constitutes the major storage proteins in hempseed, accounting for approximately 60–80% of the total seed protein (*w*/w), which serves as the primary nitrogen reserve during fermentation (Gao et al., 2021). Similar findings were reported in previous studies, where peptides derived from hemp protein hydrolysates produced by neutral protease were also primarily sourced from cupin type-1 domain–containing proteins (Liu et al., 2025).

3.3. Prediction of potential bioactive peptides

PeptideRanker was employed to predict the potential bioactive peptides in each sample (Fig. 2d). Peptides with a PeptideRanker score above 0.5 were considered bioactive (Zhao et al., 2024), detailed information for these sequences is provided in Table S1. Consistent with the overall peptide distribution, the BS group exhibited the highest number of predicted bioactive peptides, followed by the LR and AN group. Among all samples, BSH showed the highest number of bioactive peptides (463). In the AN and BS groups, higher DH was associated with an increased number of potentially bioactive peptides, whereas the opposite trend was observed in the LR group. Interestingly, although LRH exhibited a relatively lower total number of potentially bioactive peptides, it showed the highest proportion of potentially bioactive peptides relative to the total identified peptides (40.95%). This suggests that while extensive proteolysis in the LRH group may reduce total peptide diversity, it may selectively enrich the fraction of sequences with high predicted biological potential.

To further investigate the functional potential of the identified peptidome, sequences with relative abundance greater than 1% were analyzed using the BIOPEP-UWM database (Minkiewicz et al., 2019). The top five most abundant peptides from each sample are summarized in Table 4. In the unfermented control (CON), peptide diversity was limited, with the dominant peptide LWHHTFYNELR accounting for 58.3% of the total peptide area. Fermented groups exhibited a more balanced and diverse peptide distribution, reflecting extensive proteolysis.

Analysis by matching amino acids sequence using the BIOPEP-UWM database suggested that many of these high-abundance peptides contain fragments that potentially possess multiple bioactivities, including antioxidant (▲), ACE-inhibitory (■), and DPP-IV inhibitory (○) activities (Table 4). These *in silico* predictions provide preliminary insights into the multi-functional nature of the peptides and serve as a supportive screening tool to guide further functional validation. High-abundance peptides in the fermented samples frequently exhibited all three predicted activities simultaneously. The distinct profiles observed among starter cultures, such as the prevalence of DLVSP and GLHLP in the AN group, FSGF and NLPLL in the BS group, and FDERLR and FHLA in the LR group, underscore the substrate specificity and unique cleavage preferences of each microbial proteolytic system. Furthermore, the enrichment of these predicted antioxidant and enzyme inhibitory peptides is consistent with subsequent biochemical assay results, supporting the efficacy of fermentation in enhancing the functional properties of hempseed cake. Both PeptideRanker and BIOPEP-UWM predicted potential peptide bioactivity based on amino acid sequence; therefore, further validation using molecular docking was performed, as described in Section 3.4.

3.4. Molecular docking of ACE and DPP-IV with selected peptides

To explore potential interaction modes between peptides and target enzymes, the five most abundant peptides from each sample were subjected to molecular docking against ACE and DPP-IV. This was employed as a qualitative tool to provide structural insights into peptide–enzyme interactions rather than to quantitatively predict inhibitory efficacy. Docking scores are summarized in Table 4, where lower scores indicate stronger binding affinity for the active site. Several high-abundance peptides failed to produce stable binding poses within the defined sites and were subsequently excluded.

ACE plays a central role in blood pressure regulation by converting angiotensin I into the vasoconstrictor angiotensin II and degrading the vasodilator bradykinin (Xue et al., 2021). ACE-inhibitory peptides can competitively block this enzyme, exhibiting potential inhibitory activities. Among the docked sequences, FHLA (LRL/H), LFNP (ANH), LDVSP (ANL), and LVSPL (BSL/H) exhibited the strongest binding, with docking scores of −8.77, −8.65, −8.03, and − 6.89 kcal/mol, respectively. The 2D interaction diagrams (Fig. 3) reveal that these peptides interact significantly with the three major active site pockets: S1 (Ala354, Glu384, Tyr523), S2 (Gln281, His353, Lys511, His513, Tyr520), and S1′ (Glu162) (Dong et al., 2024). All four lead peptides interacted with residues in the S1 and S2 pockets, notably forming hydrogen bonds with Gln281 and Lys511. These patterns are consistent with the known binding features of ACE-inhibitory peptides. For instance, LVSPL formed additional hydrogen bonds with Ala354 and His513, which likely contributed to its favorable docking score.

DPP-IV rapidly inactivates incretin hormones, such as glucagon-like peptide-1 (GLP-1), which impairs insulin secretion and postprandial glucose regulation. Inhibiting DPP-IV prolongs incretin activity and may

Table 4
Top 5 abundant peptides in unfermented and fermented hempseed cake, their predicted bioactivities according to the BIOPEP-UWM database and molecular docking score.*

Sample	Peptide Sequence	Peak area	Ratio	Bioactivity of peptide fragments	Docking score (kcal/mol)	
					ACE	DPP-IV
CON	LWHHTFYNELR	1.85E+08	58.3	▲■○		
	SGFDTRLL	25,574,379	8.1	▲■○		−7.42
	LSMHHTFYNELR	24,918,690	7.9	▲■○		
	LWHHTFYDQLR	14,390,064	4.5	▲■○		
	FVGHHTFYNELR	13,130,846	4.1	▲■○		
ANL	**DLVSP**	3.81E+09	17.1	■○	−7.82	−6.25
	DDRNSLLR	2.02E+09	9.1	▲■○		**−9.49**
	LDVSP	1.98E+09	8.9	■○	**−8.03**	−6.90
	GVADW	9.81E+08	4.4	■○	−3.89	−8.08
	GQNDDRNSLLR	8.68E+08	3.9	▲■○		
ANH	GLHLP	5.13E+09	12.8	▲■○	−4.34	−6.34
	LHLP	2.81E+09	7.0	▲■○	−7.50	−6.17
	LFNP	2.57E+09	6.4	■○	**−8.65**	−6.69
	GNLF	1.27E+09	3.2	■○	−7.76	**−8.03**
	NDDRNSLLR	8.9E+08	2.2	▲■○		−6.69
BSL	**FSGF**	1.65E+09	7.9	■○	−6.74	−5.51
	LVSPL	1.09E+09	5.2	■○	**−6.89**	**−8.20**
	LFSGF	1.03E+09	4.9	■○	−3.03	−6.70
	LFTT	9.22E+08	4.4	■○	−4.87	−7.16
	DTRLL	8.59E+08	4.1	■○	−3.88	−5.63
BSH	**NLPLL**	5.36E+09	9.8	▲■○	−2.37	−5.69
	FSGF	4.84E+09	8.8	■○	−6.74	−5.51
	LVSPL	4.03E+09	7.4	■○	**−6.89**	**−8.20**
	SVLY	2.6E+09	4.8	▲■○	−6.70	−6.81
	LFTT	1.85E+09	3.4	■○	−4.87	−7.16
LRL	FDERLR	2.61E+09	7.1	▲■○		**−7.94**
	FHLA	2.47E+09	6.7	■○	**−8.77**	−6.26
	LFTT	1.51E+09	4.1	▲■○	−4.87	−7.16
	AFGALS	1.39E+09	3.8	■○	−2.75	−7.79
	VLLAF	1.35E+09	3.7	▲■○		−7.63
LRH	**FHLA**	1.56E+09	8.6	▲■○	**−8.77**	−6.26
	AFGALS	9.83E+08	5.4	▲■○	−2.75	**−7.79**
	SVGGLLQ	8.75E+08	4.8	■○		−5.14
	SVNLLQ	6.88E+08	3.8	■○		−7.32
	QLDDNPRRFY	6.68E+08	3.7	▲■○		

* Abbreviations (CON, ANL, ANH, BSL, BSH, LRL, LRH) are defined in Table 1. The bioactivity of peptide fragments was determined using the 'profiles of potential bioactivity' tool in the BIOPEP-UWM database. Symbols represent the presence of one or more active motifs within the parent sequence: ▲ represents antioxidant activity, ■ represents ACE-inhibitory activity, and ○ represents DPP-IV inhibitory activity. Bolded peptide sequences indicate peptides sharing within the same starter culture (Table S2). A = alanine, C = cysteine, D = aspartic acid, E = glutamic acid, F = phenylalanine, G = glycine, H = histidine, K = lysine, L = leucine, M = methionine, N = asparagine, P = proline, Q = glutamine, R = arginine, S = serine, T = threonine, V = valine, W = tryptophan, Y = tyrosine. Missing values represent unsuccessful docking attempts.

improve glycemic control (Wang et al., 2024). Therefore, DPP-IV inhibitory peptides are significant candidates for functional foods with potential glucose-regulating activities. Among the identified peptides, DDRNSLLR (ANL), GNLF (ANH), LVSPL (BSL/H), FDERLR (LRL), and AFGALS (LRH) exhibited the strongest binding affinities toward DPP-IV, with docking scores of −9.49, −8.03, −8.20, −7.94, and − 7.79 kcal/mol, respectively (Table 4). DPP-IV contains two key catalytic binding pockets: the hydrophobic S1 pocket (Ser630, Asp708, His740, Tyr547, Tyr631, Trp659, Val656, Tyr662, Tyr666, Asn710, and Val711) and the charged S2 pocket (Arg125, Glu205, Glu206, Val207, Ser209, Arg358, and Phe357) (Wang et al., 2024). The 2D docking interactions are illustrated in Fig. 4. Notably, DDRNSLLR formed a π–π stacking interaction with Tyr666 and multiple hydrogen bonding with Arg358, Ser209, and Glu205. These extensive interactions at both the catalytic and peripheral residues likely account for its superior binding affinity. By contrast, AFALS formed only a single hydrogen bond (Glu205) and one π–π interaction (Tyr666), resulting in comparatively weaker binding.

3.5. Validation of synthesized peptide

To validate the *in silico* predictions and docking results, eight representative peptides identified from the fermented hempseed cake were synthesized for *in vitro* bioactivity assays. The inhibitory potencies, expressed as IC_{50} values, are summarized in Fig. 5. As illustrated in Fig. 5a, the selected peptides displayed varying degrees of ACE inhibitory potential. LDVSP emerged as the most potent inhibitor with an IC_{50} value of 107.47 ± 6.57 μM, followed by LVSPL (127.06 ± 12.11 μM) and LFNP (145.67 ± 13.53 μM). The superior inhibitory activity of LDVSP and LVSPL is consistent with the general structure-activity requirements for ACE inhibitors, which favor peptides containing hydrophobic residues, particularly C-terminal proline (P), known to promote high-affinity interactions with the ACE active-site pockets (S1 and S2) (Ding et al., 2023). Notably, although FHLA showed the highest theoretical affinity in molecular docking (Section 3.4), its inhibitory potency in the biochemical assay was low (IC_{50} = 271.96 ± 27.02 μM ($p < 0.05$)). This discrepancy suggests that while FHLA can theoretically form stable hydrogen bonds with Gln281 and Lys511, the sequence orientation might limit its effective binding compared to the more flexible pentapeptides like LDVSP.

Regarding DPP-IV inhibition (Fig. 5b), LVSPL was the most effective inhibitor with a significantly low IC_{50} value of 2.21 ± 0.04 mM ($p < 0.05$) compared to others. This high potency aligns with the presence of valine (V) at the second N-terminal position and a hydrophobic cluster including proline (P), both of which are key structural motifs recognized by the DPP-IV catalytic site (Mu et al., 2024). In contrast, DDRNSLLR and GNLF exhibited the lowest inhibitory potential (11.74 ± 1.30 mM and 15.68 ± 0.77 mM, respectively), despite DDRNSLLR's superior

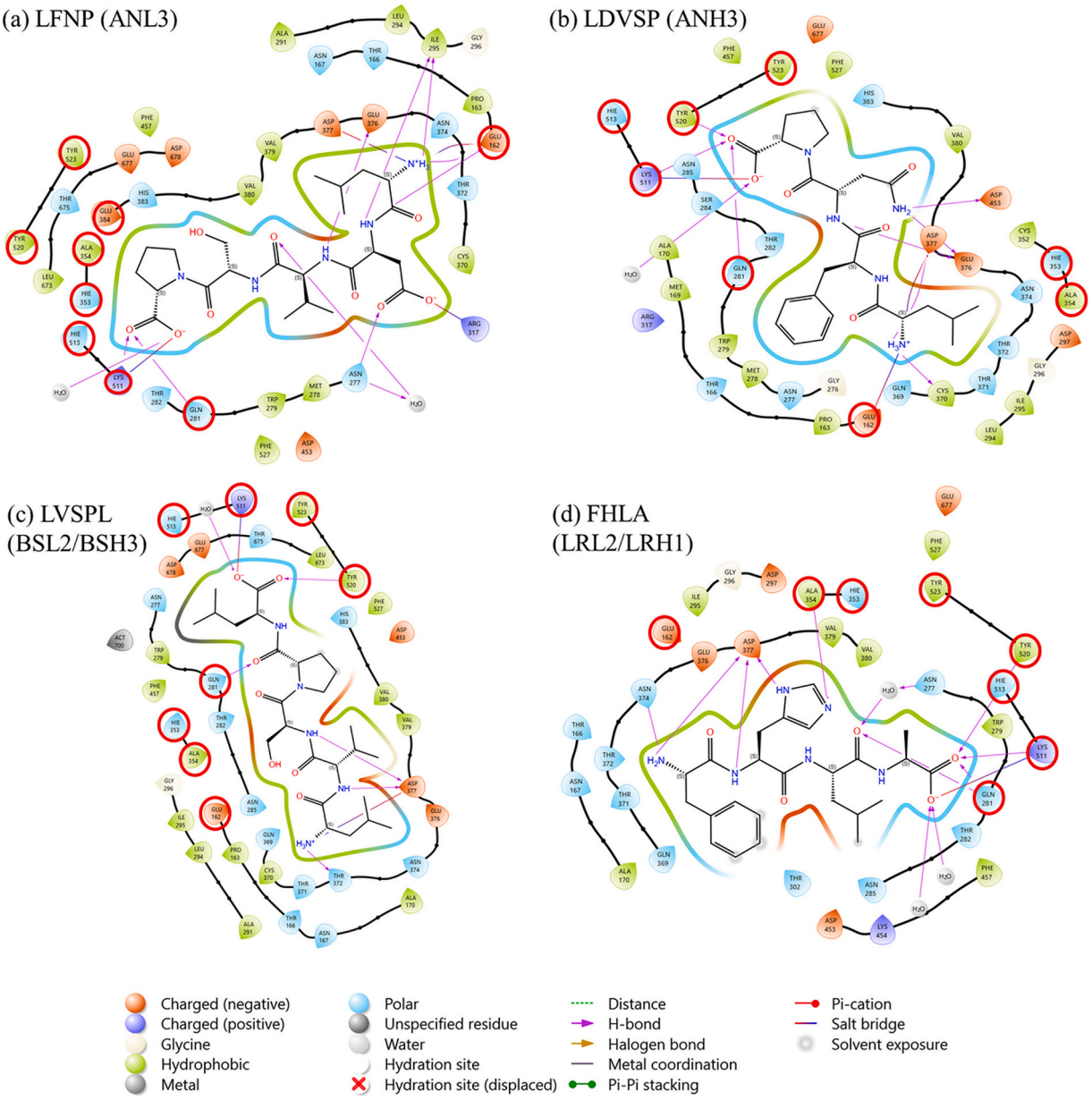

Fig. 3. Two-dimensional molecular docking diagrams of peptides (a) LFNP, (b) LDVSP, (c) LVSPL, and (d) FHLA with ACE (PDB ID: 1O8A). The source of each peptide is indicated in parentheses. Abbreviations ANL/H, BSL/H, and LRL/H are defined in Table 1. The red circle highlights the ACE active binding site. (For interpretation of the references to colour in this figure legend, the reader is referred to the web version of this article.)

docking score. This confirms that for longer octapeptides, theoretical binding energy may not fully account for the accessibility of the peptide to the enzyme's catalytic site *in vitro* due to the steric hindrance.

Interestingly, LVSPL demonstrated multifunctional properties by simultaneously inhibiting both ACE and DPP-IV. This bifunctionality is likely driven by its balanced hydrophobic profile and the strategic positioning of the proline residue, which satisfies the binding requirements of both enzymes.

The inhibitory potencies of these fermentation-induced hempseed peptides are competitive when compared to previously reported hempseed peptides. Although the IC_{50} of LDVSP (107.47 μM) is weaker than the well-known hempseed derived ACE inhibitory peptide WVYY (27 μM) (Girgih et al., 2014) but its inhibition is comparable to or superior than other peptides such as LGV (145 μM) (Orio et al., 2017) and WYT (574 μM) (Girgih et al., 2014). Similarly, the IC_{50} of LVSPL for DPP-IV inhibition (2.21 mM, approx. 1.17 mg/mL) is stronger than TNGPQLIH (1.7 mg/mL) released from Flavourzyme-hydrolyzed hempseed protein (Amigo-Benavent et al., 2026). These comparisons validate that SSF of hempseed cake is an effective strategy for generating high-value multifunctional peptides. However, while these peptides demonstrated potent *in vitro* activities, their bioaccessibility remains to be further validated in future studies to account for the potential impact of proteolysis during gastrointestinal digestion.

3.6. Antioxidant activity of fermented hempseed cake

Antioxidant activities of unfermented and fermented hempseed cakes (both total soluble protein and their <3 kDa peptide fraction) were evaluated by the ABTS radical scavenging and FRAP assays (Fig. 6a–d). Both assays showed similar trends. At a standardized concentration of 1 mg/mL, <3 kDa fraction shows higher antioxidant potential and the unfermented hempseed cake (CON) exhibited significantly higher ($p < 0.05$) antioxidant activity than the fermented groups (Fig. 6a, c). This may be due to the higher content of predicted antioxidant sequences in

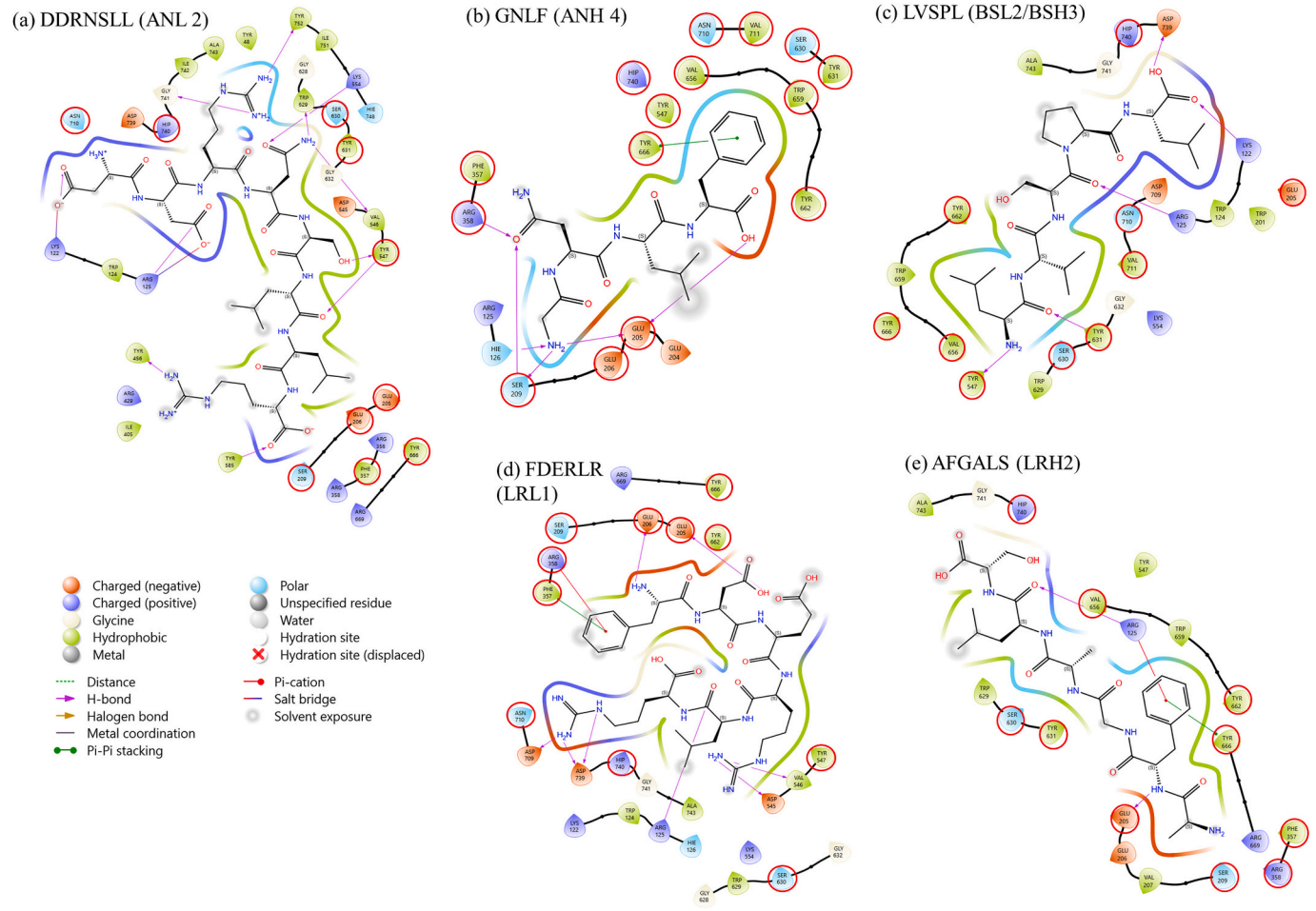

Fig. 4. Two-dimensional docking diagrams of peptides (a) DDRNSLL, (b) GNLF, (c) LVSPL, (d) FDERLR and (e) AFGALS with DPP-IV (PDB: 4A5S). The source of each peptide is indicated in parentheses. Abbreviations ANL/H, BSL/H, and LRL/H are defined in Table 1. The red circle highlights the DPP-IV active binding site. (For interpretation of the references to colour in this figure legend, the reader is referred to the web version of this article.)

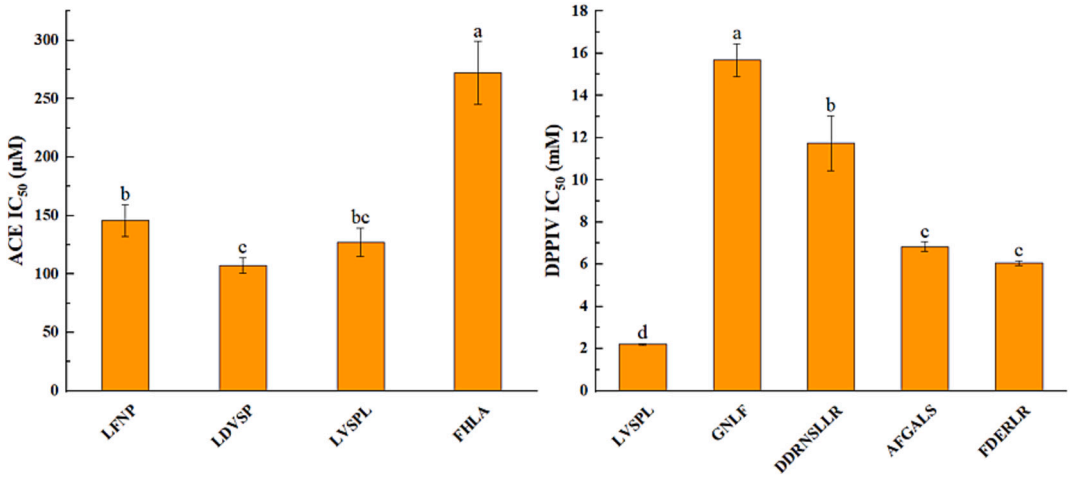

Fig. 5. Inhibitory activities of the selected synthetic peptides against target enzymes. (a) IC_{50} values of peptides for angiotensin-converting enzyme (ACE) inhibition. (b) IC_{50} values of peptides for dipeptidyl peptidase-IV (DPP-IV) inhibition. Bars (mean ± standard deviation, $n = 3$) with different letters are significantly different at $p < 0.05$.

CON (84.5%) compared to fermented samples (16.4–35%) (Table S2). Similar findings have been reported where enzymatic hydrolysis of hemp protein isolate with alcalase and bromelain led to a decrease in specific radical scavenging activity (Hong et al., 2022). Additionally, The consistently higher antioxidant activity of the <3 kDa fractions compared to total protein extracts aligns with previous findings that smaller hemp peptides exhibit superior radical scavenging and electron-donating capacities due to their enhanced reactivity (Agrawal et al.,

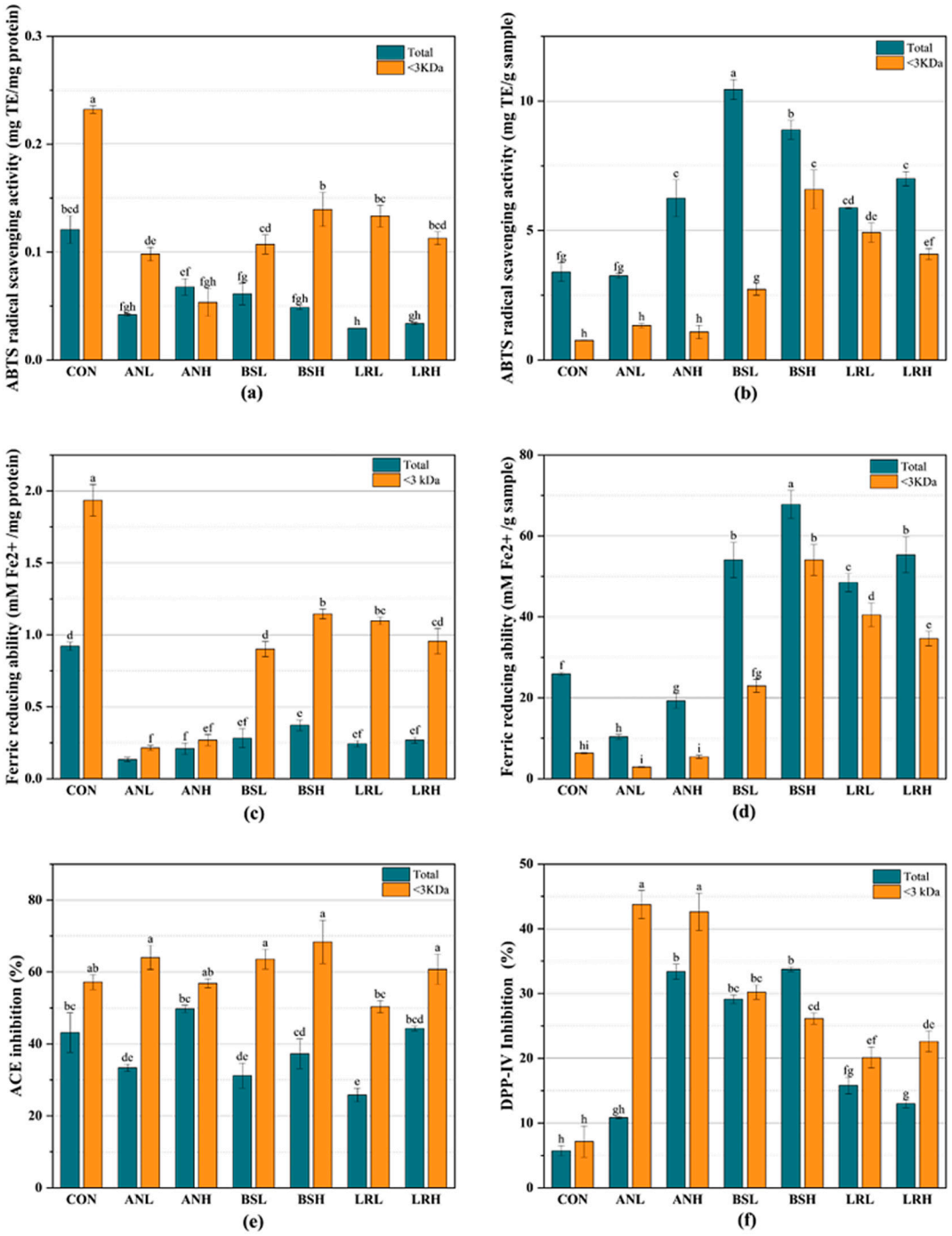

Fig. 6. *In vitro* antioxidant and enzyme inhibitory activities of unfermented and fermented hempseed cake protein extracts. (a, b) ABTS radical scavenging activity and (c, d) ferric reducing antioxidant power (FRAP), expressed at 1 mg/mL protein concentration (a, c) and normalized to sample weight (b, d). (e) Angiotensin-I-converting enzyme (ACE) inhibitory activity and (f) dipeptidyl peptidase IV (DPP-IV) inhibitory activity, both measured at 1 mg/mL protein concentration. Data are presented as mean ± standard deviation ($n = 3$). Different lowercase letters indicate significant differences between samples ($p < 0.05$).

2019; Girgih, Udenigwe, & Aluko, 2011).

However, solid-state fermentation significantly increased the yield of soluble protein, thereby enhancing the total amount of bioactive peptides extractable from the same substrate (Table 2). When antioxidant activity was expressed per gram of sample, the fermented groups exhibited substantially higher antioxidant activity compared with the CON (Fig. 6b, d), with BSL showing the highest ABTS radical scavenging activity (10.44 mg TE/g sample), and BSH exhibiting the highest FRAP value (67.77 mM Fe^{2+}/g sample). The superior performance of the BS groups suggests that the choice of starter culture is a primary determinant of antioxidant potential, consistent with observations in fermented soybean (Hou et al., 2023).

3.7. ACE inhibitory activity of fermented hempseed cake

The ACE inhibitory activities of the total soluble protein extracts and the <3 kDa peptide fractions at 1 mg/mL are presented in Fig. 6e. All samples demonstrated ACE inhibition, and the <3 kDa peptide fractions exhibited significantly enhanced inhibitory activity compared to the total soluble protein extracts. This suggests that smaller peptides are

generally more effective ACE inhibitors than their larger counterparts. Among the treatments, the BS and AN groups yielded the highest results. Specifically, the <3 kDa BSH and ANL fractions exhibited the highest inhibition (68.37% and 64.02%, respectively). First, these results are consistent with the specific peptide analysis detailed in Section 3.5, where LDVSP (IC_{50} = 107.47 ± 6.57 μM, identified in ANL) and LVSPL (127.06 ± 12.11 μM, identified in BSH) emerged as the most potent inhibitor. Second, the high activity in these groups correlates with a higher proportion of peptides possessing favorable terminal motifs. ACE-inhibitory peptides typically favor peptides with proline (P) at the C-terminus and Leucine (L) at the N-terminus (Ding et al., 2023). In this study, the ANL group possessed the highest C-terminal Proline ratio of 25.3% (Fig. 2b), while the BSH group exhibited the highest N-terminal Leucine ratio of 33.5% (Fig. 2b).

Although no significant differences ($p > 0.05$) were observed between the unfermented and fermented samples when normalized to protein content, the overall ACE-inhibitory capacity per gram of hempseed cake increased significantly after fermentation (Feng et al., 2025). This improvement is primarily driven by the significantly elevated yield of soluble peptides in the fermented substrate. While ACE-inhibitory peptides have previously been isolated from hempseed protein *via* enzymatic hydrolysis (Girgih et al., 2014; Girgih, Udenigwe, Li, et al., 2011; Orio et al., 2017), SSF represents a novel bioprocessing approach for their generation. Notably, previously identified hemp-derived ACE-inhibitory peptides, such as GVLY, IEE, LGV, and RVR (Orio et al., 2017), were absent in the present study. This discrepancy is likely due to the distinct proteolytic patterns of microbial enzymes compared to standard commercial proteases. The peptides identified in this study, specifically LDVSP, LFNP, LVSPL, and FHLA, not only exhibited strong molecular docking scores (Table 4) but were also experimentally validated (IC_{50}) in Section 3.5. These results confirm that SSF is a highly effective bioprocessing strategy for releasing novel and potent ACE-inhibitory sequences from the hempseed protein matrix.

3.8. DPP-IV inhibitory activity of fermented hempseed cake

The DPP IV inhibitory activities of total soluble proteins and the <3 kDa peptides fractions (at 1 mg/mL) are presented in Fig. 6f. Compared with the unfermented control (CON, 5.72%), all fermented samples exhibited significantly enhanced activity ($p < 0.05$). The <3 kDa AN group showing the highest inhibition (ANL 43.75%, ANH 42.62%).

Interestingly, while experimental validation in Section 3.5 identified the BS-derived pentapeptide LVSPL as the single most potent inhibitor (IC_{50} = 2.21 mM), the AN group maintained superior total inhibitory activity. This apparent discrepancy suggests that the high bioactivity of the AN extract is driven by its overall peptidomic landscape rather than the dominance of a single sequence. Peptidomic mapping (Fig. 2b) revealed that compared to the BS and LR groups, the AN group possesses a higher density of peptides containing C-terminal proline residues (25% in ANL and 19.8% in ANH, compared to 9.5% and 10.7% of BS group and 6.0 and 5.7 in LR group), a structural feature known to enhance DPP-IV inhibitory potential (Nongonierma & FitzGerald, 2013).

Beyond peptides, the metabolic shifts during SSF including changes in free amino acids and organic acids, may also contribute to the observed enzyme inhibition. Therefore, the bioactivity of the fermented extracts likely reflects the effect of multiple fermentation-derived components.

4. Conclusion

This study demonstrates that solid-state fermentation of hempseed cake with *A. niger*, *B. subtilis*, and L. *rhamnosus* effectively enhanced protein hydrolysis and the generation of low-molecular-weight peptides (<3 kDa). The resulting peptide profiles and bioactivities were significantly influenced by both the starter culture and the degree of hydrolysis. Among the tested strains, *B. subtilis* fermentation generated the highest overall peptide abundance and antioxidant activity, whereas extracts fermented with *A. niger* exhibited the strongest DPP-IV inhibitory activity. Peptidomic analysis provided peptide-level insight, revealing that most peptides originated from Cupin type-1 proteins (Edestin) and that microbial cleavage favored sequences containing motifs associated with antioxidant, ACE-inhibitory, and DPP-IV inhibitory activities. Through a combined *in silico* and *in vitro* approach, representative peptides were further evaluated using synthesized standards, confirming that LDVSP and LVSPL possessed ACE inhibitory activity. Notably, LVSPL also displayed potential multifunctional bioactivity by inhibiting both ACE and DPP-IV. These findings highlight SSF as a sustainable bioprocessing strategy for the targeted production of high-value functional ingredients, though further research is required to evaluate the gastrointestinal stability and bioavailability of these peptides.

CRediT authorship contribution statement

Xiaoyu Feng: Writing – review & editing, Writing – original draft, Visualization, Software, Methodology, Formal analysis, Data curation, Conceptualization. **Pangzhen Zhang:** Writing – review & editing, Supervision. **Ken Ng:** Writing – review & editing, Supervision. **Said Ajlouni:** Writing – review & editing, Supervision. **Zijian Liang:** Visualization, Software, Methodology. **Zhongxiang Fang:** Writing – review & editing, Resources, Project administration, Funding acquisition, Conceptualization.

Funding

This study was funded by AgriFutures Australia.

Declaration of competing interest

The authors declare that they have no known competing financial interests or personal relationships that could have appeared to influence the work reported in this paper.

Acknowledgements

The authors acknowledge the use of mass spectrometry facilities at the Bio21 Mass Spectrometry and Proteomics Facility (MSPF), Bio21 Molecular Science and Biotechnology Institute, University of Melbourne. This research was made possible through the financial support of AgriFutures Australia as part of the Emerging Industries Australian Hemp Industry Program of Research – Theme 3, Project 3.1, to improve the health and nutritional value of hemp oil cake protein by fermentation. The authors would like to thank Southern Cross University for their role in managing the Australian Industrial Hemp Program of research and Charles Sturt University for their role in project management. We extend our gratitude to the Melbourne research scholarship of the University of Melbourne Scholarship.

Appendix A. Supplementary data

Supplementary data to this article can be found online at https://doi.org/10.1016/j.foodchem.2026.149243.

Data availability

Data will be made available on request.

References

Agrawal, H., Joshi, R., & Gupta, M. (2019). Purification, identification and characterization of two novel antioxidant peptides from finger millet (eleusine coracana) protein hydrolysate. *Food Research International, 120*, 697–707. https://doi.org/10.1016/j.foodres.2018.11.028

Alabdalall, A. H., Al-Anazi, N. A., Aldakheel, L. A., Amer, F. H., Aldakheel, F. A., Ababutain, I. M., … Al-Khaldi, E. M. (2021). Application and characterization of crude fungal lipases used to degrade fat and oil wastes. *Scientific Reports, 11*(1), 19670. https://doi.org/10.1038/s41598-021-98927-4

Amadou, I., Kamara, M. T., Tidjani, A., Foh, M., & Le, G. (2010). Physicochemical and nutritional analysis of fermented soybean protein meal by lactobacillus plantarum lp6. *World Journal of Dairy & Food Sciences, 5*(2), 114–118.

Amigo-Benavent, M., Rivero-Pino, F., Villanueva-Lazo, A., Montserrat-de la Paz, S., FitzGerald, R. J., & Millan-Linares, M. C. (2026). Identification, characterization and resistance to digestion assessment of hemp-derived dipeptidyl-peptidase IV inhibitory peptides. *Food & Function, 17*(1), 577–587. https://doi.org/10.1039/D5FO02421H

Burley, S. K., Berman, H. M., Bhikadiya, C., Bi, C., Chen, L., Di Costanzo, L., … Dutta, S. (2019). RCSB protein data bank: Biological macromolecular structures enabling research and education in fundamental biology, biomedicine, biotechnology and energy. *Nucleic Acids Research, 47*(D1), D464–D474. https://doi.org/10.1093/nar/gky1004

Cano, A., Hernández-Ruíz, J., García-Cánovas, F., Acosta, M., & Arnao, M. B. (1998). An end-point method for estimation of the total antioxidant activity in plant material. *Phytochemical Analysis: An International Journal of Plant Chemical and Biochemical Techniques, 9*(4), 196–202. https://doi.org/10.1002/(SICI)1099-1565(199807/08)9:4<196::AID-PCA395>3.0.CO;2-W

Chen, H., Xu, B., Wang, Y., Li, W., He, D., Zhang, Y., … Xing, X. (2023). Emerging natural hemp seed proteins and their functions for nutraceutical applications. *Food Science and Human Wellness, 12*(4), 929–941. https://doi.org/10.1016/j.fshw.2022.10.016

Chen, H.-H., Li, W., Wang, Y., Xu, B., Hu, X., Li, X.-B., … Xing, X.-H. (2023). Mining and validation of novel hemp seed-derived DPP-IV-inhibiting peptides using a combination of multi-omics and molecular docking. *Journal of Agricultural and Food Chemistry, 71*(23), 9164–9174. https://doi.org/10.1021/acs.jafc.3c00535

Contesini, F. J., Melo, R. R.d., & Sato, H. H. (2018). An overview of *Bacillus* proteases: From production to application. *Critical Reviews in Biotechnology, 38*(3), 321–334. https://doi.org/10.1080/07388551.2017.1354354

David Troncoso, F., Alberto Sánchez, D., & Luján Ferreira, M. (2022). Production of plant proteases and new biotechnological applications: An updated review. *ChemistryOpen, 11*(3), Article e202200017. https://doi.org/10.1002/open.202200017

Ding, Q., Sheikh, A. R., Chen, Q., Hu, Y., Sun, N., Su, X., … He, R. (2023). Understanding the mechanism for the structure-activity relationship of food-derived ACEI peptides. *Food Reviews International, 39*(4), 1751–1769. https://doi.org/10.1080/87559129.2021.1936005

Dong, Y., Yan, W., Zhang, Y.-Q., & Dai, Z.-Y. (2024). A novel angiotensin-converting enzyme (ACE) inhibitory peptide from tilapia skin: Preparation, identification and its potential antihypertensive mechanism. *Food Chemistry, 430*, 137074. https://doi.org/10.1016/j.foodchem.2023.137074

Dunwell, J. M., Khuri, S., & Gane, P. J. (2000). Microbial relatives of the seed storage proteins of higher plants: Conservation of structure and diversification of function during evolution of the cupin superfamily. *Microbiology and Molecular Biology Reviews, 64*(1), 153–179. https://doi.org/10.1128/mmbr.64.1.153-179.2000

Feng, X., Ng, K., Ajlouni, S., Zhang, P., & Fang, Z. (2024). Effect of solid-state fermentation on plant-sourced proteins: A review. *Food Reviews International, 40*(9), 2580–2617. https://doi.org/10.1080/87559129.2023.2274490

Feng, X., Ng, K., Ajlouni, S., Zhang, P., Liang, Z., & Fang, Z. (2025). Enhancement of protein hydrolysis and bioactivity in hempseed cake via solid-state fermentation using *Aspergillus niger*, *Bacillus subtilis*, and *Lactobacillus rhamnosus*. *Food and Bioprocess Technology*, 1–19. https://doi.org/10.1007/s11947-025-03940-4

Gao, J., Li, T., Chen, D., Gu, H., & Mao, X. (2021). Identification and molecular docking of antioxidant peptides from hemp seed protein hydrolysates. *Lwt, 147*, Article 111453. https://doi.org/10.1016/j.lwt.2021.111453

Garcia, F. L., Ma, S., Dave, A., & Acevedo-Fani, A. (2021). Structural and physicochemical characteristics of oil bodies from hemp seeds (cannabis sativa l.). *Foods, 10*(12), 2930. https://doi.org/10.3390/foods10122930

Girgih, A. T., He, R., & Aluko, R. E. (2014). Kinetics and molecular docking studies of the inhibitions of angiotensin converting enzyme and renin activities by hemp seed (cannabis sativa l.) peptides. *Journal of Agricultural and Food Chemistry, 62*(18), 4135–4144. https://doi.org/10.1021/jf5002606

Girgih, A. T., Udenigwe, C. C., & Aluko, R. E. (2011). In vitro antioxidant properties of hemp seed (cannabis sativa l.) protein hydrolysate fractions. *Journal of the American Oil Chemists' Society, 88*(3), 381–389. https://doi.org/10.1007/s11746-010-1686-7

Girgih, A. T., Udenigwe, C. C., Li, H., Adebiyi, A. P., & Aluko, R. E. (2011). Kinetics of enzyme inhibition and antihypertensive effects of hemp seed (cannabis sativa l.) protein hydrolysates. *Journal of the American Oil Chemists' Society, 88*(11), 1767–1774. https://doi.org/10.1007/s11746-011-1841-9

Griffin, S. P., & Bhagooli, R. (2004). Measuring antioxidant potential in corals using the FRAP assay. *Journal of Experimental Marine Biology and Ecology, 302*(2), 201–211. https://doi.org/10.1016/j.jembe.2003.10.008

Hong, S., Lin, Y., & Dia, V. P. (2022). Anti-inflammatory and antioxidant properties of hempseed protein enzymatic hydrolysates. *Food Hydrocolloids for Health, 2*, Article 100082. https://doi.org/10.1016/j.fhfh.2022.100082

Hou, H., Zhou, W., Guo, L., Jia, S., Zhang, X., & Wang, L. (2023). Effects of characteristics of douchi during rapid fermentation and antioxidant activity using different starter cultures. *Journal of the Science of Food and Agriculture, 103*(5), 2459–2472. https://doi.org/10.1002/jsfa.12419

House, J. D., Neufeld, J., & Leson, G. (2010). Evaluating the quality of protein from hemp seed (cannabis sativa l.) products through the use of the protein digestibility-corrected amino acid score method. *Journal of Agricultural and Food Chemistry, 58*(22), 11801–11807. https://doi.org/10.1021/jf102636b

Krishna, C. (2005). Solid-state fermentation systems—An overview. *Critical Reviews in Biotechnology, 25*(1–2), 1–30. https://doi.org/10.1080/07388550590925383

Kumari, R., Sharma, N., Sharma, S., Samurailatpam, S., Padhi, S., Singh, S. P., & Rai, A. K. (2023). Production and characterization of bioactive peptides in fermented soybean meal produced using proteolytic bacillus species isolated from kinema. *Food Chemistry, 421*, Article 136130. https://doi.org/10.1016/j.foodchem.2023.136130

Leonard, W., Zhang, P., Ying, D., Xiong, Y., & Fang, Z. (2021). Effect of extrusion technology on hempseed (cannabis sativa l.) oil cake: Polyphenol profile and biological activities. *Journal of Food Science, 86*(7), 3159–3175. https://doi.org/10.1111/1750-3841.15813

Liang, Z., Zhang, P., Ma, W., Zeng, X.-A., & Fang, Z. (2024). Physicochemical properties, antioxidant activities and comprehensive phenolic profiles of tea-macerated chardonnay wine and model wine. *Food Chemistry, 436*, Article 137748. https://doi.org/10.1016/j.foodchem.2023.137748

Liu, M.-Q., Zhao, H.-F., Zhao, Z.-Y., Zhang, Y.-H., & Dong, Y. (2025). Preparation, identification and potential mechanism of novel urate-lowering active peptide from hemp protein: From animal model to computer simulation. *Food Research International.* , Article 116643. https://doi.org/10.1016/j.foodres.2025.116643

Minkiewicz, P., Iwaniak, A., & Darewicz, M. (2019). BIOPEP-UWM database of bioactive peptides: Current opportunities. *International Journal of Molecular Sciences, 20*(23), 5978. https://doi.org/10.3390/ijms20235978

Mooney, C., Haslam, N. J., Pollastri, G., & Shields, D. C. (2012). Towards the improved discovery and design of functional peptides: Common features of diverse classes permit generalized prediction of bioactivity. *PLoS One*. https://doi.org/10.1371/journal.pone.0045012

Mu, X., Wang, R., Cheng, C., Ma, Y., Zhang, Y., & Lu, W. (2024). Preparation, structural properties, and in vitro and in vivo activities of peptides against dipeptidyl peptidase IV (DPP-IV) and α-glucosidase: A general review. *Critical Reviews in Food Science and Nutrition, 64*(27), 9844–9858. https://doi.org/10.1080/10408398.2023.2217444

Nongonierma, A. B., & FitzGerald, R. J. (2013). Inhibition of dipeptidyl peptidase IV (DPP-IV) by proline containing casein-derived peptides. *Journal of Functional Foods, 5*(4), 1909–1917. https://doi.org/10.1016/j.jff.2013.09.012

Norris, R., Poyarkov, A., O'Keeffe, M. B., & FitzGerald, R. J. (2014). Characterisation of the hydrolytic specificity of aspergillus Niger derived prolyl endoproteinase on bovine β-casein and determination of ACE inhibitory activity. *Food Chemistry, 156*, 29–36. https://doi.org/10.1016/j.foodchem.2014.01.056

Novelli, P. K., Barros, M. M., & Fleuri, L. F. (2016). Novel inexpensive fungi proteases: Production by solid state fermentation and characterization. *Food Chemistry, 198*, 119–124. https://doi.org/10.1016/j.foodchem.2015.11.089

Orio, L. P., Boschin, G., Recca, T., Morelli, C. F., Ragona, L., Francescato, P., … Speranza, G. (2017). New ACE-inhibitory peptides from hemp seed (cannabis sativa l.) proteins. *Journal of Agricultural and Food Chemistry, 65*(48), 10482–10488. https://doi.org/10.1021/acs.jafc.7b04522

Oyeleke, S. B., Oyewole, O. A., & Egwim, E. C. (2011). Production of protease and amylase from bacillus subtilis and aspergillus Niger using parkia biglobossa (africa locust beans) as substrate in solid state fermentation. *Advances in Life Sciences, 1*(2), 49–53.

Pandey, A. (2003). Solid-state fermentation. *Biochemical Engineering Journal, 13*(2–3), 81–84. https://doi.org/10.1016/S1369-703X(02)00121-3

Solieri, L., De Vero, L., & Tagliazucchi, D. (2018). Peptidomic study of casein proteolysis in bovine milk by lactobacillus casei PRA205 and lactobacillus rhamnosus PRA331. *International Dairy Journal, 85*, 237–246. https://doi.org/10.1016/j.idairyj.2018.06.010

Sonklin, C., Alashi, M. A., Laohakunjit, N., Kerdchoechuen, O., & Aluko, R. E. (2020). Identification of antihypertensive peptides from mung bean protein hydrolysate and their effects in spontaneously hypertensive rats. *Journal of Functional Foods, 64*, Article 103635. https://doi.org/10.1016/j.jff.2019.103635

Sutton, J. M., Clark, D. E., Dunsdon, S. J., Fenton, G., Fillmore, A., Harris, N. V., … MacKenzie, R. E. (2012). Novel heterocyclic DPP-4 inhibitors for the treatment of type 2 diabetes. *Bioorganic & Medicinal Chemistry Letters, 22*(3), 1464–1468. https://doi.org/10.1016/j.bmcl.2011.11.054

Wang, C., Zheng, L., Udenigwe, C. C., Lin, L., & Zhao, M. (2024). Molecular mechanistic insights into dipeptidyl peptidase-IV inhibitory peptides to decipher the structural basis of activity. *Journal of Agricultural and Food Chemistry, 72*(19), 11230–11240. https://doi.org/10.1021/acs.jafc.3c08791

Wang, P., & Ma, T. (2024). Production of bioactive peptides from tartary buckwheat by solid-state fermentation with lactiplantibacillus plantarum ATCC 14917. *Foods, 13*(19), 3204. https://doi.org/10.3390/foods13193204

Wang, X., Chen, H., Fu, X., Li, S., & Wei, J. (2017). A novel antioxidant and ACE inhibitory peptide from rice bran protein: Biochemical characterization and molecular docking study. *Lwt, 75*, 93–99. https://doi.org/10.1016/j.lwt.2016.08.047

Wang, X.-S., Tang, C.-H., Yang, X.-Q., & Gao, W.-R. (2008). Characterization, amino acid composition and in vitro digestibility of hemp (cannabis sativa l.) proteins. *Food Chemistry, 107*(1), 11–18. https://doi.org/10.1016/j.foodchem.2007.06.064

Wei, G., Regenstein, J. M., & Zhou, P. (2021). The fermentation-time dependent proteolysis profile and peptidomic analysis of fermented soybean curd. *Journal of Food Science, 86*(8), 3422–3433. https://doi.org/10.1111/1750-3841.15823

Wu, J. Y., Wee, S., Ler, S. G., Henry, C. J., & Gunaratne, J. (2025). Unraveling the impact of tempeh fermentation on protein nutrients: An *in vitro* proteomics and peptidomics approach. *Food Chemistry, 474*, Article 143154. https://doi.org/10.1016/j.foodchem.2025.143154

Xie, Y., Wang, J., Wang, S., He, R., Wang, Z., Zhao, L., & Ge, W. (2024). Preparation, characterization, and mechanism of DPP-IV inhibitory peptides derived from bactrian camel milk. *International Journal of Biological Macromolecules, 277*, Article 134232. https://doi.org/10.1016/j.ijbiomac.2024.134232

Xue, L., Yin, R., Howell, K., & Zhang, P. (2021). Activity and bioavailability of food protein-derived angiotensin-I-converting enzyme–inhibitory peptides. *Comprehensive Reviews in Food Science and Food Safety, 20*(2), 1150–1187. https://doi.org/10.1111/1541-4337.12711

Yu, X., Chen, Y., Qi, Z., Chen, Q., Cao, Y., & Kong, Q. (2023). Preparation and identification of a novel peptide with high antioxidant activity from corn gluten meal. *Food Chemistry, 424*, Article 136389. https://doi.org/10.1016/j.foodchem.2023.136389

Yu, Y., Yu, W., & Jin, Y. (2021). Peptidomic analysis of milk fermented by *Lactobacillus delbrueckii* subsp. *bulgaricus* and *Streptococcus thermophilus*. *Food Hydrocolloids for Health, 1*, Article 100033. https://doi.org/10.1016/j.fhfh.2021.100033

Zhang, J., Xin, L., Shan, B., Chen, W., Xie, M., Yuen, D., … Ma, B. (2012). PEAKS DB: De novo sequencing assisted database search for sensitive and accurate peptide identification. *Molecular and Cellular Proteomics, 11*(4). https://doi.org/10.1074/mcp.M111.010587

Zhang, Y., Zhang, C., Zhu, S., Wang, J., Li, H., & Liu, X. (2023). Identification and characterization of soybean peptides and their fractions used by lacticaseibacillus rhamnosus lra05. *Food Chemistry, 401*, Article 134195. https://doi.org/10.1016/j.foodchem.2022.134195

Zhao, J., Kong, X., Zhang, C., Hua, Y., Chen, Y., & Li, X. (2024). *In vitro* protein digestive properties and peptidomic characterization of five whole component plant protein beverages using a pepsin-pancreatin model. *Food Research International, 196*, Article 115076. https://doi.org/10.1016/j.foodres.2024.115076